section for Cl^- and I^- are in good agreement with the theory.

One might also look at the I^- photodetachment cross-section measurements of Steiner.[7] We see very good agreement between the experimental shape and the calculated shape[4] of the cross section, but a large disagreement (a factor of 2) in its absolute magnitude.

ACKNOWLEDGMENTS

The author wishes to thank B. Kival and E. Evans who were involved in some of the initial phases of this work. Also acknowledged is the assistance from R. Taylor, K. Wray, and J. D. Teare. The technical assistance from J. W. Martz, Jr., in the operation of the shock tube was a most important contribution to this program.

†Research supported by the Advanced Research Projects Agency of the Department of Defense and Space and Missile Systems Organization, Air Force Systems Command, and was monitored by Space and Missile Systems Organization, Air Force Systems Command, under Contract No. F04701-70-C-0128.

[1]M. S. Vadya, Mem. Roy. Astron. Soc. 71, 249 (1967).

[2]L. M. Branscomb, Ann. Geophys. 20, 88 (1964).

[3]J. W. Cooper and J. B. Martin, Phys. Rev. 126, 1482 (1962).

[4]E. J. Robinson and S. Geltman, Phys. Rev. 153, 4 (1967).

[5]Y. V. Moskvin, Teplofiz. Vys. Temp. 3, 821 (1965), [High Temp. 3, 765 (1965)].

[6]B. Steiner, M. L. Seman, and L. M. Branscomb, J. Chem. Phys. 37, 1200 (1962).

[7]B. Steiner, Phys. Rev. 173, 136 (1968). This paper has a good bibliography of recent photodetachment cross-section publications.

[8]D. E. Roethe, Phys. Rev. 177, 93 (1969).

[9]R. S. Berry and C. W. Reimann, 38, 1540 (1963). The author has become aware of a more recent measurement of the threshold absorption of F^- made by H.-P. Popp, Z. Naturforsch. 22a, 254 (1967). He finds values somewhat lower than ours but consistent with them for the quoted experimental uncertainties.

[10]R. S. Berry, T. Cernoch, M. Coplan, and J. J. Ewing, J. Chem. Phys. 49, 127 (1968); J. J. Ewing, R. M. Stein, and R. S. Berry, in the Seventh Shock Tube Symmposium, Toronto, Canada, 1969 (unpublished).

[11]We measured both the ablation and dissociation times of CsF separately and found that these times were typically a few microseconds. It can be shown that these measured ablation times correspond to particle sizes of less than 1μ. Results of these measurements will be published elsewhere.

[12]A. Mandl, B. Kivel, and E. Evans, J. Chem. Phys. (to be published).

[13]A. Mandl, E. Evans, and B. Kivel, Chem. Phys. Letters 5, 307 (1970). Preliminary results for collisional detachment of F^- by Ar and Cs^+.

[14]L. Agnew and C. Summers, in *Proceedings of the Seventh International Conference on Ionization Phenomena in Gases, Belgrade*, 1965, edited by B. Perovic and D. Tosić (Gradjevinska Knjiga Publishing House, Belgrade, Yugoslavia, 1966).

[15]S. M. Gridneva and G. A. Kasabar, High Temp. 9, 651 (1969) .

[16]D. W. Norcross and P. M. Stone, J. Quant. Spectrosc. Radiat. Transfer 6, 277 (1966).

[17]D. E. Rothe, J. Quant. Spectrosc. Radiat. Transfer 9, 49 (1969).

[18]R. L. Taylor and G. Caledonia, J. Quant. Spectrosc. Radiat. Transfer 9, 657 (1969).

[19]H. Mirels, Phys. Fluids 6, 1201 (1963); 9, 1265 (1966); 9, 1907 (1966).

PHYSICAL REVIEW A VOLUME 3, NUMBER 1 JANUARY 1971

Electronic Recombination of He_3^+†

J. B. Gerardo and M. A. Gusinow
Sandia Laboratories, Albuquerque, New Mexico 87115
(Received 21 May 1970)

The electronic recombination coefficient of He_3^+ under thermalized conditions at 80 °K is $(3.4 \pm 1.5) \times 10^{-6}$ cm^3 sec^{-1}. The electron-temperature dependence of this coefficient is $T_e^{-\chi}$, $\langle\chi\rangle = 1.22$, $0.98 < \chi < 1.60$. This is applicable when both the gas and ion temperatures are near 80 °K. The fragments of the recombination process have not been identified but the results indicate dissociation into $He_2^* + He$.

I. INTRODUCTION

Recently, Patterson[1] identified in a drift tube filled with helium an ion which had the following properties: (i) a dissociation energy of 0.172 eV; (ii) formation from He_2^+ with a rate coefficient greater than 1.7×10^{-31} cm^6 sec^{-1} at 76 °K; and (iii) stability at gas temperatures < 200 °K. These observations suggested that the ion in question was the triatomic ion He_3^+. Subsequently, a mass-12 ion was observed in a "relatively clean" 80 °K helium flowing afterglow plasma by Ferguson *et al.*[2] Later, deVries and Oskam[3] conclusively showed by isotope studies in a cataphoretically pure helium afterglow that $^4He_3^+$ ($A = 12$) and $^4He_4^+$ ($A = 16$) are both stable at temperatures near 80 °K. At the present time the

molecular structures of He_3^+ and He_4^+ are not known.

This study is concerned with an experimental determination of the rate at which free electrons recombine with He_3^+. The study was performed with gas and ion temperatures near 80 °K and electron temperatures between 80 and 300 °K. The electron temperature T_e was elevated above the gas temperature by application of a moderately intense microwave field. The recombination coefficient was deduced from measurements of the electron density measured by conventional microwave (low power) transmission techniques. At low values of gas pressure, mass analysis (including isotope studies) was used to determine the relative concentrations of He^+, He_2^+, He_3^+, and He_4^+.

Microwave studies of afterglow helium plasmas with gas temperatures near 80 and 4 °K were previously reported by Kaplafka *et al.*[4] and Goldan *et al.*[5] Our observations are consistent with these previous studies but our interpretation of the observed phenomena differs from theirs substantially.

II. EXPERIMENTAL APPARATUS

The plasma was formed in a quartz discharge tube (8 mm i.d. and 60 cm in length) which was located in a U-shaped section of H-band (2.85 cm $\times$1.26 cm i.d.) waveguide. This assembly could be placed in a Dewar filled with liquid N_2. Tantalum electrodes were fastened to the discharge tube by glass side tubes located near each end of the discharge tube. The electrode side tubes protruded through 4-mm-diam holes in the center plane of the broad wall of the waveguide. These side tubes were sealed to the metal walls of the guide with silicone rubber adhesive to prevent liquid N_2 from entering the waveguide. The section of waveguide located in the liquid N_2 was flushed with helium and pressurized to prevent condensation of water vapor on the walls of the guide and discharge tube.

The discharge tube was evacuated by means of a conventional stainless-steel and glass vacuum system equipped with an oil diffusion pump and bakeable to 300 °K. The tantalum electrodes were outgassed under vacuum with a high-power rf field. The base vacuum, measured near the discharge tube, was typically 10^{-9} Torr while connected to the pumping station and when disconnected increased with an initial rate of about 10^{-8} Torr/h attaining a final pressure of $\sim 2\times10^{-8}$ Torr after several hours. The evacuated discharge tube was filled with cataphoretically pure helium and the pressure was measured with a calibrated Baratron capacitance manometer.

Optical radiation from the plasma was transmitted to a grating spectrometer by fiber light pipes. The atomic line and molecular band radiation was detected with fast photomultipliers and the temporally resolved photon count was recorded with a multichannel analyzer. This sensitive detection system could resolve several individual lines and bands for times up to several milliseconds into the afterglow.

The microwave system which was used to heat the free electrons and diagnose the electronic properties of the plasma is illustrated in Fig. 1. The sensing microwave signal, frequency f_s, was of sufficiently low power (~ 10 μW) to cause negligible heating of the free electrons.[6] The frequency of this microwave field was typically 8.3 GHz but several frequencies from 8.1 to 10.0 GHz were used to determine reliability and also to search for possible systematic errors in the measurements. The amplitude of the heating signal (frequency f_h, nominally 9.0 GHz) was variable to a maximum value of 130 mW (peak electric field of 8.22 V/cm).

The phase shift and attenuation of the sensing microwave signal as it traversed the plasma was measured by conventional microwave interferometer techniques.[7,8] The measurement requires setting ΔR and $\Delta\Phi$ to obtain a null reading on the slotted line detector and noting the change in each due to introduction of the plasma. The phase shift was, in practice, measured by movement of the micrometer drive slotted line detector rather than the calibrated phase shifter. This practice was followed because phase shifters introduce an insertion loss in the system which varies slightly with setting and thus prevents measurement of absorptivity of the plasma to the desired accuracy. The stub tuners on each side of the slotted line were positioned to minimize reflections in this section of waveguide.

The phase shift $\Delta\Phi$ and attenuation ΔdB of the sensing wave as it traverses the section of waveguide containing the plasma are functions of the free-electron density N_e, the electron-collision fre-

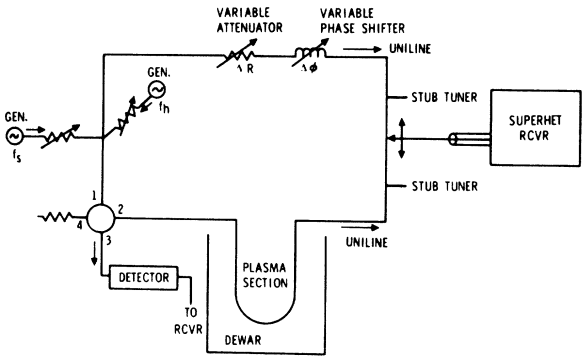

FIG. 1. Microwave system used in this study. The discharge tube was located in a U-shaped section of waveguide which could be completely submerged in the liquid nitrogen filled Dewar.

quency for momentum transfer ν and the velocity distribution function of the free electrons. The relationships have been derived previously[9] but to the knowledge of the authors they do not appear in open literature in the form used here. For this reason their derivation is outlined in the Appendix and the results are given by

$$\bar{\nu}_r = 41.4\ \Delta\mathrm{dB}\, f_s\, \frac{1}{\Delta\Phi^0}\,, \tag{1}$$

$$N_e = \frac{2m\epsilon_0\lambda_s^2\omega_s^2\Delta\Phi^0}{\xi e^2\lambda_{g0} l\ 360}\left[1+\left(\frac{\bar{\nu}_r}{\omega_s}\right)^2\right], \tag{2}$$

where $\bar{\nu}_r$ is an effective electron-collision frequency,[10] $\omega_s = 2\pi f_s$, $\lambda_s = c/f_s$, and all other symbols are defined in the Appendix. The effective collision frequency $\bar{\nu}_r$ for helium is given by Eq. (A3) in the Appendix. The collision frequency for momentum transfer is defined by

$$\nu = \int QNVf(V)\, d^3\vec{v}\,, \tag{3}$$

where N is the gas density. If the cross section Q is assumed constant and equal to 5.6×10^{-16} cm^2,[11] an effective electron temperature is obtained using Eq. (3) and the relationship between ν and $\bar{\nu}_r$ [Eq. (A3)]. Thus, if $\bar{\nu}_r \ll \omega$,

$$T_e^* = 2.95\times10^{-16}\,(\bar{\nu}_r/p)^2\,[1+0.124\,(\bar{\nu}_r/\omega)^2]^2\ ^\circ\mathrm{K}, \tag{4}$$

where p is the background gas pressure in Torr. A Maxwellian velocity distribution at a temperature T_e^* was assumed in arriving at Eq. (4). Measured values of $\bar{\nu}_r$ were substituted into the equation to evaluate the electron temperature T_e both with and without a heating microwave field. The estimated accuracy of this measurement will be discussed in some detail in Sec. VI.

When an ionized gas is subjected to a microwave field, the velocity distribution and the average energy of the free electrons are altered. Margenau[6] showed that the increase in temperature ΔT_e for a field strength E is given by

$$\Delta T_e = \frac{2}{3k}\left(\frac{M}{4\omega^2}\right)\left(\frac{eE}{m}\right)^2 \quad \text{for } \Delta T_e \leq T_g\,, \tag{5}$$

where M is the molecular weight of the gas. Equation (5) was derived under conditions of $\omega \gg \nu$ and the absence of inelastic collisions. Margenau also showed that the distribution function remains essentially Maxwellian if the field strength is sufficiently weak to satisfy $\Delta T_e \leq T_g$. Frommhold *et al.*[12] extended Margenau's analysis for the case $\Delta T_e > T_g$ and $Q(V) = \text{const}$. It was shown that in this case, the distribution function remains close to Maxwellian for ΔT_e less than several T_g. Frommhold *et al.* modified Eq. (5) by including a multiplicative factor $F(Z)$, where

$$Z = (\omega^2 m/NQeE)\,(3m/M)^{1/2}\,.$$

Their tabulated values of $F(Z)$ indicate that under the conditions of this experiment $F(Z)$ is equal to 0.8 or greater.

A block diagram of the electrical circuitry is illustrated in Fig. 2. The master generator was used to initiate a periodic discharge at a predetermined rate (usually 30 cps). The discharge pulse was nominally 20 kV in amplitude and 2 μsec wide. The results reported here are independent of either of these parameters or on the discharge repetition rate.

The plasma was also mass analyzed with a quadrupole mass filter by observing the ion currents through a small hole in the wall of the discharge tube. Ion counts as a function of time in the afterglow were recorded with a multichannel analyzer operated in the multiscaling mode. Due to the complexity of both the microwave circuitry and the mass spectrometer, it was not possible to make simultaneous measurements or even measurements on the same discharge tube. Thus, there is some question concerning direct temporal comparison of the microwave and mass spectrometer results because the initial plasma in the discharge tubes may not be the same. Only those mass spectrometer results which are applicable to this study will be mentioned here.

III. PHENOMENOLOGICAL DISCUSSION OF OBSERVATIONS

All observations were made during the afterglow period and at times greater than the time required for T_e to fall to near 80 °K (as indicated by the collision frequency measurements). Microwave interferometric measurements and observations of optical radiation from the plasma yielded results typified by the illustrations in Fig. 3. These re-

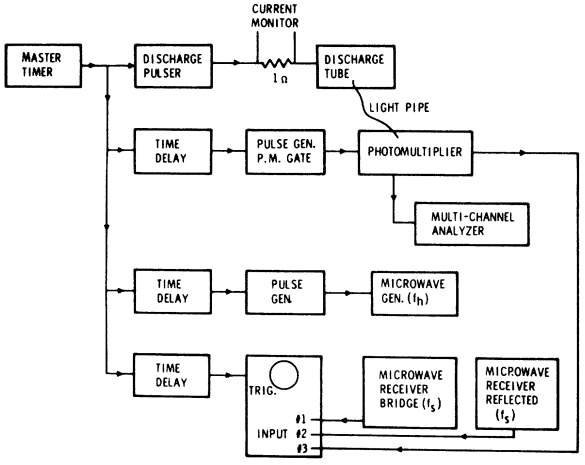

FIG. 2. Block diagram of electrical circuitry.

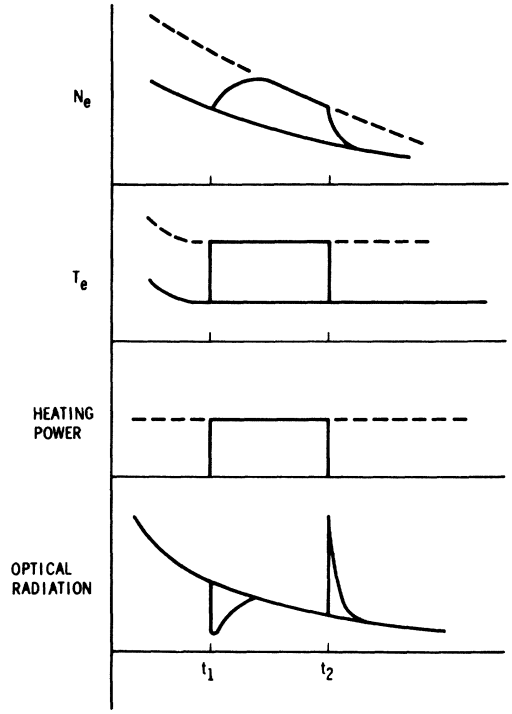

FIG. 3. General behavior of the plasma parameters with pulsed and continuous microwave heating. The dashed lines indicate the behavior with application of continuous microwave heating. The solid lines indicate the behaviors when both pulsed heating or no heating wave is incident on the plasma. Steady-state behavior is regained upon termination of the heating wave in a few tenths of a microsecond.

sults are essentially the same as observed previously by Kaplafka *et al.*[4] and in part by Goldan *et al.*[5] The phenomenon with which this study is most concerned is the rapid rise of N_e following application of the heating wave and the rapid decrease of N_e when the heating wave is suddenly terminated. The percent change of N_e increased monotonically with increased microwave heating power. Following the transient ($t \gg t_1$), the electron density is identical to the value of $N_e(t)$ attained when a heating wave of equal intensity is operated continuously. Upon termination of the heating wave at $t = t_2$, the value of N_e falls to its nonheated value in a few tenths of a microsecond.

Molecular band radiation dominated the plasma emission at all times except during the very early afterglow. Atomic radiation from principal quantum levels greater than $n = 4$ was essentially absent after the first few hundred microseconds of the afterglow period. Insofar as this study is concerned, the most essential aspect of the optical emission was the observation that the intensity of a given band, or atomic line, was the same with continuous microwave heating as it was in the absence of heating. When a pulsed heating wave was applied, the intensity, after the initial transient, was independent of the level of heating and equal to the intensity when no heating wave was applied.

Kaplafka *et al.*[4] concluded that the increase in N_e following application of a heating wave could be attributed to a T_e-dependent source term for free electrons. Without going into details, we contend that this conclusion is not entirely consistent with the observations. In Sec. IV a model is discussed which includes a T_e-independent source term for free electrons but a loss term which is inversely dependent on T_e. While absolute proof of the present model is lacking, we show that it is consistent with our observations in every respect. It is then shown that quantitative measurement of the recombination loss term is possible by observation of the phenomena discussed above, and thus we arrive at a value for the electron-ion recombination coefficient. Under proper conditions this recombination coefficient can be assigned to He_3^+.

IV. PLASMA MODEL

The continuity equations for electrons, metastable atoms, He^*, He_2^+, and He_3^+ are listed in Eqs. (6),

$$\frac{dN_e}{dt} = -N_e \sum_i \alpha_i [He_i^+] - \sum_i \frac{D_{ai}}{\Lambda^2} [He_i^+] + \tfrac{1}{2}\beta [M]^2 , \tag{6a}$$

$$\frac{d[M]}{dt} = -\beta [M]^2 - Ap^2 [M] - \frac{D_M}{\Lambda^2} [M] + N_e \sum_i f_i \alpha_i [He_i^+] , \tag{6b}$$

$$\frac{d[He^*]}{dt} = -\frac{D_{a1}}{\Lambda^2} [He^*] + \tfrac{1}{2}\beta [M]^2 - k_1 p^2 [He^*] - \alpha_1 N_e [He^*] , \tag{6c}$$

$$\frac{d[He_2^+]}{dt} = -\frac{D_{a2}}{\Lambda^2} [He_2^+] + k_1 p^2 [He^*] - k_2 p^2 [He_2^+] - \alpha_2 N_e [He_2^+] , \tag{6d}$$

$$\frac{d[He_3^+]}{dt} = -\frac{D_{a3}}{\Lambda^2} [He_3^+] + k_2 p^2 [He_2^+] - \alpha_3 N_e [He_3^+] + \text{loss}. \tag{6e}$$

The [ ] are used to indicate densities of the quantity specified by the enclosed symbol; M represents

atomic metastables; p is gas pressure; D_{ai} is ambipolar diffusion coefficient of ion i; Λ is the characteristic diffusion length (fundamental mode is assumed); α_i is the recombination coefficient of ion i; and A, β, k_1, and k_2 are appropriate conversion rates. The last term on the right-hand side of Eq. (6b) is included to account for recycling (that is, metastable atoms produced by the recombination process). The f_i coefficients are the fraction of ith-type ions which terminate as atomic metastables when they recombine. The loss term in Eq. (6e) is included to account for collisional destruction of He_3^+. Accepted values for several of the coefficients used in Eqs. (6) are listed in Table I along with appropriate references. The listed references should not be construed as complete but only representative.

The time constant for conversion of He^+ to He_2^+ at 80 °K is

$$(k_1 p^2)^{-1} = 3.8\times10^{-4} p^{-2} \text{ sec}$$

or less than 4×10^{-6} sec for p greater than 10 Torr. The time constant for subsequent conversion to He_3^+ is less than this value.[1] The relative densities of He_3^+ and He_2^+ can be estimated by assuming that Eq. (6e) is in a quasisteady state. At gas pressures of a few Torr or more and N_e typical of the values attained in this investigation, the recombination loss of He_3^+ was found to be much larger than the diffusive loss. Thus,

$$[He_3^+]/[He_2^+] \approx k_2 p^2/\alpha_3 N_e > 6.6\times10^8 N_e^{-1} p^2 ;$$

at $N_e = 10^{10}$ cm^{-3}, $p = 10$ Torr, this ratio is greater than 6. The recombination coefficient used in this evaluation is the value determined in this study. Confirmation of the relative concentrations of He_3^+ and He_2^+ by mass spectroscopy at a pressure of 10 Torr and higher is complicated by possible break up of the marginally bound He_3^+ as it passes through the sampling hole. On the spectrometer side of the sampling hole, the gas density is relatively high and the ions are accelerated by an applied electric field. Consequently, collisional destruction of marginally bound ions may be significant when the gas pressure in the discharge vessel is high. Mass spectroscopy results were obtained which indicate that $[He_3^+]/[He_2^+] > 1$ for $t > 700$ μsec (time referenced with respect to initiation of the discharge) and $p > 10$ Torr, but the exact value of this ratio varies with the time in the afterglow. The quasisteady state concentration ratio evaluated above using the previously determined value[1] for k_2 is used as the principal argument that He_3^+ is the dominant ion at high gas pressure.

Considering each term in Eqs. (6a) and (6b), and retaining only the dominant terms, these two equations reduce approximately to the following (under the conditions of this experiment $\Lambda^2 = 0.0276$ cm^2, $N_e > 10^9$ cm^{-3}, $M > 5\times10^{10}$ cm^{-3}):

$$\frac{dN_e}{dt} = \dot{N}_e = -\alpha^* N_e^2 + \tfrac{1}{2}\beta[M]^2 , \tag{7a}$$

$$\frac{d[M]}{dt} = -\beta[M]^2 - \frac{D_M}{\Lambda^2}[M] , \tag{7b}$$

where

$$\alpha^* N_e^2 = N_e \textstyle\sum_i \alpha_i [He_i^+].$$

Neglect of ambipolar diffusion compared to recombination is justified by the results of this study. The production of atomic metastables M via the recombination processes is neglected because they will result mainly from recombination of atomic ions He^+ and this represents a negligible fraction of the net recombination. Dissociative recombination of He_2^+ can lead to an atomic metastable but the cross section for this recombination is believed to be negligible. Dissociative recombination of He_3^+ could lead to either an atomic or a molecular metastable state. The fraction of these events which terminate to atomic metastables is believed to be small by the results of this study. This will be discussed in Sec. VI.

The additional plasma condition most favorable to a study of $e - He_3^+$ recombination would be a negli-

TABLE I. Relevant coefficients.

	$T_g = 300$ °K		$T_g = 77$ °K	
	Value	Reference	Value	Reference
β	2×10^{-9} cm^3 sec^{-1}	13		
A	0.2 sec^{-1} Torr^{-2}	13	3×10^{-3} sec^{-1} Torr^{-2}	13
$D_M P$	500 cm^2 sec^{-1}	14	42 cm^3 sec^{-1}	14
$D_{a1}p$	$225(1+T_e/T_g)$ cm^2 sec^{-1}	15	$22.9(1+T_e/T_g)$ cm^2 sec^{-1}	15
$D_{a2}p$	$353(1+T_e/T_g)$ cm^2 sec^{-1}	15	$23.6(1+T_e/T_g)$ cm^2 sec^{-1}	15
$D_{a3}p$			$25.6(1+T_e/T_g)$ cm^2 sec^{-1}	15
k_1	1.08^{-31} cm^6 sec^{-1}	16	1.7×10^{-31} cm^6 sec^{-1}	1
k_2			$>1.7\times10^{-31}$ cm^6 sec^{-1}	1
α_1	$\alpha_1(N_e, T_e)$	17		
α_2	$\alpha_2(N_e, p)$	18		

gible source term in Eq. (7a), $\frac{1}{2}\beta[M]^2$. However, due to the extremely long lifetime of helium metastable atoms, this condition could not be obtained experimentally. In spite of this we will show that α^* can be deduced by observing changes in $\dot{N}_e$ which result from alterations in the value of α^* (via T_e). This is most easily illustrated by making the additional (although not necessary) assumption that Eq. (7a) is essentially in a quasisteady state (qss) (i.e., $\alpha^* N_e^2 \approx \frac{1}{2}\beta[M]^2 = S \gg \dot{N}_e$). In this case, if α^* is suddenly decreased, N_e will increase until the right-hand side of Eq. (7a) is again balanced. If α^* is subsequently increased back to its original value, then N_e will return to the same value it would have attained had α^* not been altered. This behavior is similar to that depicted in Fig. 3 which can be explained with the above model simply by assuming that S is independent of T_e and that α^* is inversely dependent on T_e^x. Both of these assumptions are not only plausible but are probable. Thus, considering Fig. 3, the increase in $\dot{N}_e$ at $t = t_1^+$ is indicative of the decrease in α^* at $t = t_1$ and the decrease in $\dot{N}_e(t = t_2^+)$ is indicative of the increase in α^* at $t = t_2$.

The temporal behavior of the electron density at $t > t_1$, t_2 can be obtained from the solution of Eqs. (7) if qss is assumed. In order to illustrate this, let α_0 and α_h represent α^* at the electron temperatures T_{e0} and T_{eh}, respectively (where T_{eh} is the elevated electron temperature during microwave heating). Referring to Fig. 3, let $N_{e0}(t)$ represent $N_e(t)$ when no microwave heating is applied and let $N_{eh}(t)$ represent $N_e(t)$ when continuous heating is applied. Consider the case where microwave heating is suddenly applied at $t = t_1$. Assume that T_e increases instantaneously and that S is constant during the subsequent rise in N_e. Solution of Eq. (7a) yields

$$N_e(t) = N_{eh}(t_1)\tanh\left[2\alpha_h N_{eh}(t_1)\,(t - t_1) + \tfrac{1}{2}\ln\left(\frac{N_{e0}(t_1) + N_{eh}(t_1)}{N_{eh}(t_1) - N_{e0}(t_1)}\right)\right], \tag{8a}$$

which has the form of the observed $N_e(t)$. A similar solution for $N_e(t)$ following removal of the heating wave at time t_2 is

$$N_e(t) = N_{e0}(t_2)\coth\left[2\alpha_0 N_{e0}(t_2)\,(t - t_2) + \tfrac{1}{2}\ln\left(\frac{N_{e0}(t_2) + N_{eh}(t_2)}{N_{eh}(t_2) - N_{e0}(t_2)}\right)\right]. \tag{8b}$$

Equations (8) imply application of the qss conditions [i.e., $S(t) = \alpha_0 N_{e0}(t) = \alpha_h N_{eh}(t)$]. Solutions similar to Eqs. (8) can be obtained without using the qss condition but a simple solution does require that S be time independent. A curve fitting procedure is used with the experimental data and Eqs. (8) to evaluate α_0 and α_h.

The recombination coefficients α_0 and α_h can also be related to the initial time rate of change of N_e at $t = t_1^+$ and $t = t_2^+$ without any assumption concerning qss. Thus Eqs. (7a) and (7b) yield the following if S is independent of both T_e and prior plasma behavior:

$$\dot{N}_e(t_1^+) - \dot{N}_{e0}(t_1) = \alpha_0 N_{e0}^2(t_1) - \alpha_h N_{e0}^2(t_1), \tag{9a}$$

$$\dot{N}_e(t_1^+) - \dot{N}_{eh}(t_1) = \alpha_h[N_{eh}^2(t_1) - N_{e0}^2(t_1)], \tag{9b}$$

$$\dot{N}_e(t_2^+) - \dot{N}_{e0}(t_2) = -\alpha_0[N_{eh}^2(t_2) - N_{e0}^2(t_2)]. \tag{9c}$$

Only initial values of experimental slopes [i.e., $\dot{N}_e(t_1^+)$ and $\dot{N}_e(t_2^+)$] are required to evaluate α_0 and α_h. In practice, initial slopes derived from experimental results will be systematically underestimated. However, iteration with the aid of Eqs. (8a) and (8b) can be used to minimize the error in the resulting α_0 and α_h.

It is shown below that the qss condition is indeed satisfied to a good approximation over a wide range of parameters in the plasma discussed here. When this condition is satisfied, the electron density is controlled by the metastable density and decreases in accordance with $[M]$ as specified by Eq. (7b). At sufficiently high gas pressure and at early times in the afterglow when the metastable concentration is high, the diffusive loss of metastable atoms can be neglected and $[M]$ decays according to Eq. (10a);

$$[M]^{-1} = [M_0]^{-1} + \beta t. \tag{10a}$$

If the qss condition is satisfied the electron density will decay according to Eq. (10b);

$$1/N_e(t) = 1/N_e(t = 0) + (2\alpha^*\beta t)^{1/2}. \tag{10b}$$

Use of Eq. (10b) and β of Table I with the experimental data yields α^*.

Caution should be employed with the application of Eq. (10b) to experimental data since it requires applicability of the qss condition. The observation that $N_e^{-1}(t)$ increases linearly with time over a finite time interval is a necessary condition for qss but this observation alone is not sufficient to show that qss is applicable. This type of data should be used only sparingly as a means to evaluate α^*, but it does afford a consistency check on the plasma model. Another consistency check on the qss condition requires evaluation of α^* by means of Eqs. (10) with a continuous microwave heating signal incident on the plasma. This yields α_h from the slope of $N_e^{-1}(t)$ which can be compared with α_0 from the slope of $N_{e0}^{-1}(t)$. The qss condition requires that

$$\alpha_0/\alpha_h = [N_{eh}(t)/N_{e0}(t)]^2$$

since S is the same in both cases.

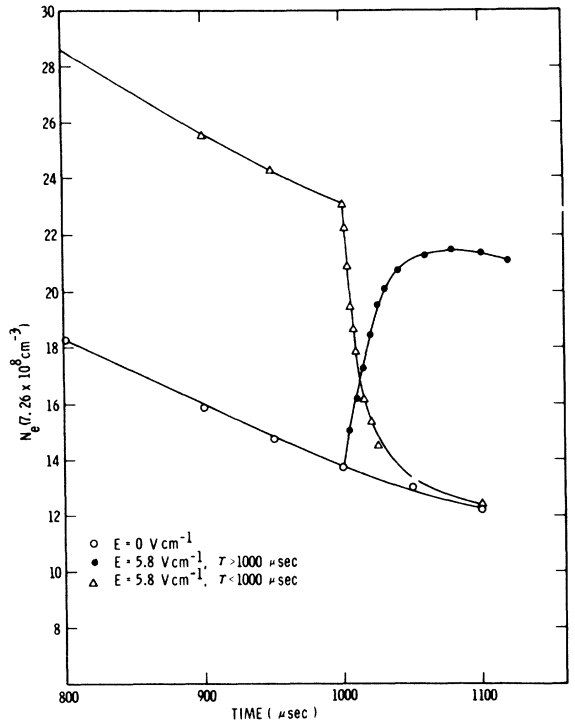

FIG. 4. Illustration of the rapid rise in N_e when a microwave field is incident on the plasma at 1000 μsec and the rapid fall when a microwave field is suddenly terminated at 1000 μsec. The background gas pressure was 30 Torr and T_e during heating was 175 °K. Typical variations of the measured values were ±2%.

V. RESULTS

Typical experimental data are illustrated in Figs. 4 and 5. Both sets of data are for 30-Torr gas pressure at a gas temperature near 80 °K. The electric field strength which was applied in each case is indicated on the figures. The bars indicated on the plots represent experimental scatter only and do not include the systematic error of the measurement. The observation that $N_e^{-1}(t)$ increased linearly with time is an indication that qss is satisfied, but this alone is not sufficient proof of the model since the range of N_e is fairly small. (See discussion in Sec. IV.)

TABLE II. Recombination coefficient for $T_e \approx 80$ °K.

	Reference	Average (10^{-6} cm^3 sec^{-1})	Standard deviation (10^{-6} cm sec^{-1})
$\alpha_0^{(1)}$	Eq. (10)	2.69	0.22
$\alpha_0^{(2)}$	Eq. (9a) (9b)	3.44	0.33
$\alpha_0^{(3)}$	Eq. (9c)	3.33	0.30

The experimentally measured effective recombination coefficient at background gas pressures up to 50 Torr and a gas temperature near 80 °K is illustrated in Fig. 6. The data is divided into two groups: $p \geq 15$ Torr and $p \leq 15$ Torr. The results in the high-pressure group are independent of both time in the afterglow ($t > 700$ μsec) and discharge conditions (voltage, pulse width, and repetition rate). The indicated values of α^* were measured by (i) the slope of $N_e^{-1}(t)$ giving α_0^1 [see Eqs. (10)]; (ii) rate of rise of N_e upon application of microwave heating giving α_0^2 [see Eqs. (9a) and (9b)]; and (iii) rate of decrease of N_e upon termination of microwave heating yielding $\alpha_0^{(3)}$. The average values of each are given in Table II. These values of $\alpha_0^{(2)}$ and $\alpha_0^{(3)}$ were arrived at by the iterative procedure discussed in Sec. IV. Typically, the iteration increased $\alpha_0^{(2)}$ by about 14% above that obtained using the initial slope only and increased $\alpha_0^{(3)}$ by about 31%.

Table II shows that $\langle \alpha_0^{(2)} \rangle$ and $\langle \alpha_0^{(3)} \rangle$ are in excellent agreement with each other but they do not overlap with $\langle \alpha_0^{(1)} \rangle$. This should not be surprising since the expected accuracy of the β coefficient used in

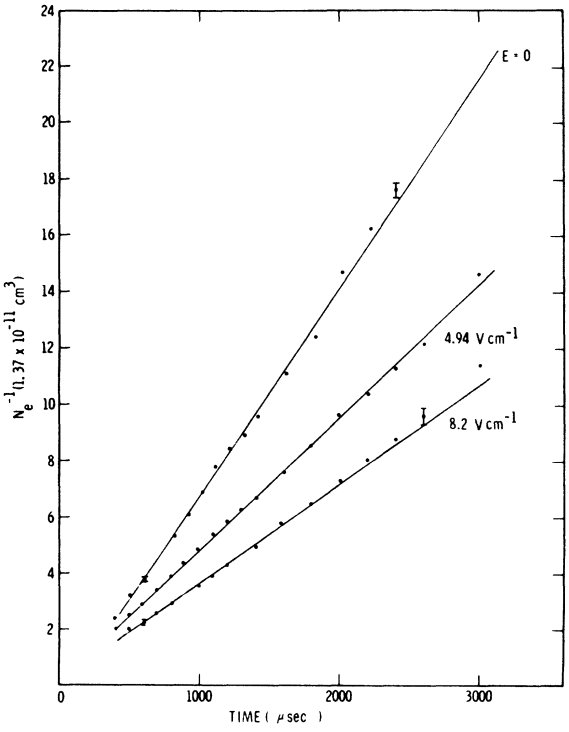

FIG. 5. Time variation of N_e^{-1} for three different values of continuous microwave heating. The gas pressure was 30 Torr. The deviation from linearity at the later times is due to non-negligible diffusive loss of atomic metastables. The bars indicate typical scatter of data.

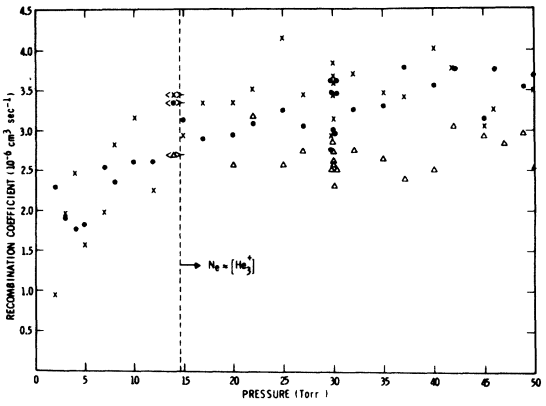

FIG. 6. Electron-ion recombination coefficient as determined at various gas pressures and a gas temperature near 80 °K. The values indicated for pressures less than 15 Torr were obtained at 1 msec in the afterglow. At pressures greater than 15 Torr the measured values were independent of time. The three symbols indicate methods of measurement: triangle, ×, dot, represent $\alpha_0^{(1)}$, $\alpha_0^{(2)}$, and $\alpha_0^{(3)}$, respectively. The average value of each is indicated to the side of the dashed vertical line.

the analysis is no better than a factor of 2.[19] The fact that $\langle \alpha_0^{(1)} \rangle$ and $\langle \alpha_0^{(2)} \rangle$ agree to within a factor of 2 illustrates once again the consistency of the proposed plasma model.

The recombination coefficient at elevated electron temperatures was measured by both pulsed microwave heating [see Eq. (9b)] and continuous heating [see Eq. (10)]. An example of the variation of the measured recombination coefficient with T_e is illustrated in Fig. 7. This set of data was obtained from the slope of $N_e^{-1}(t)$ plots with variable microwave heating power. The temperature indicated on the graphs is the effective temperature T_e^* as given by Eq. (4). It is difficult to accurately appraise the relation of T_e^* to the true T_e but there is reason to believe that they are nearly the same. This will be further discussed in Sec. VI. The results illustrated in Fig. 7 indicate that

$$\alpha = \alpha_0 \left(\frac{80}{T_e^*}\right)^{\chi}, \quad 0.98 \leq \chi \leq 1.60.$$

The main reason why the indicated range of χ is so large is due to large experimental variations in the measured T_e. Values of α for $T_e > 80$ °K were also measured with pulsed microwave heating [see Eq. (9b)] and the results are consistent with the above.

The ratio α_h/α_0 was also found to be consistent with the qss condition for gas pressures above 5 Torr and at times less than typically 2 msec into the afterglow. This was manifested by the consistent near equality of the ratios

$$\alpha_h/\alpha_0 \approx [N_{e0}(t)/N_{eh}(t)]^2.$$

This observation lends additional support for the proposed plasma model.

The reason for the falloff of α^* when the pressure is decreased to below 15 Torr is difficult to assess with confidence due to possible competing effects. On the one hand, the concentration of He_2^+ at pressures less than 10 Torr cannot be neglected in comparison with $[He_3^+]$ especially at early times in the afterglow. On the other hand, at low gas pressure it is difficult to determine that T_e is not greater than 80 °K. Measurements of T_e^* at these low pressures are complicated by appreciable reflection of the sensing microwaves by the plasma. The method of measurement used here requires that the reflection be negligible so that the insertion loss can be equated with the absorption loss. Any reflective loss that is not properly accounted for will result in a value of T_e^* larger than T_e. Calculations indicate that even at these lower pressures, T_e should be near 80 °K but the microwave measurements at low gas pressure were not sufficiently accurate to show that this is definitely true. This will be further discussed in Sec. VI.

Figure 8 illustrates α^* at a gas pressure of 5 Torr as a function of time into the afterglow. The error bars indicate reproducibility limits only and do not include systematic error. The limits are

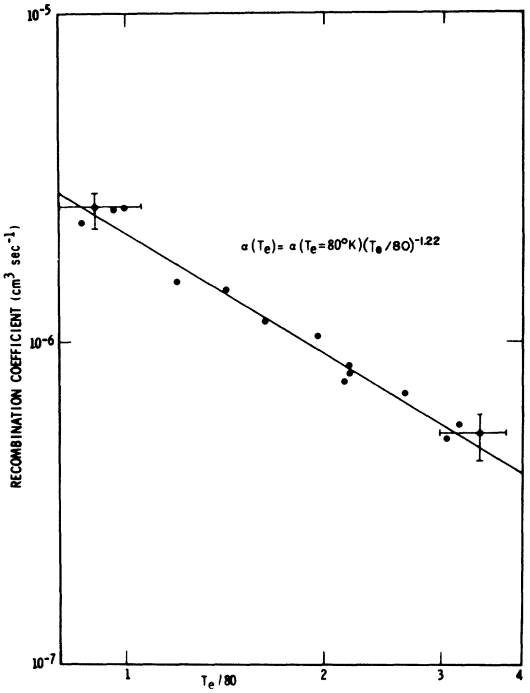

FIG. 7. Effective electron-ion recombination coefficient as determined at various values of electron temperature. The gas pressure was 30 Torr. The bars represent maximum day-to-day scatter of data.

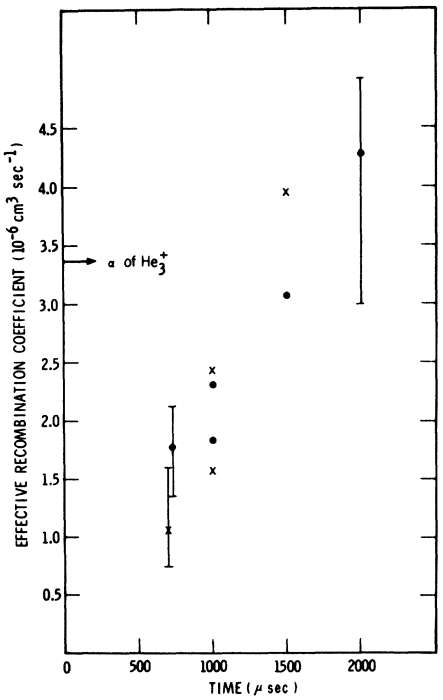

FIG. 8. Time variation of the effective electron-ion recombination coefficient as determined for a gas pressure of 5 Torr. The value of the recombination coefficient of He_3^+ at 80 °K is indicated on the left. The bars represent maximum confidence limits. The symbols indicate methods of measurement (see Fig. 6).

quite large especially at the later times when the electron density and the associated phase shift are small. At late times α^* attains a value which is not inconsistent with the recombination coefficient of He_3^+. Mass analysis of ions indicated that at 5 Torr and 700 μsec, $He_2^+ \approx He_3^+$ while at 2 msec $He_2^+ \ll He_3^+$. Thus, the results illustrated in Fig. 8 are consistent with the measured ion ratios if the recombination coefficient of He_2^+ is less than that of He_3^+, a result which might be expected. However, it is difficult to determine with conviction that the decrease of α^* at early times is not due to T_e greater than 80 °K. Figure 7 indicates that an elevated T_e could account for the measured value of α^* at 700 μsec if $T_e \approx 140$ °K. This is inconsistent with our expectations, as is discussed in Sec. VI, but it cannot be discounted with certainty.

Some ion loss-rate studies at very low pressure did indicate that for $p < 0.2$ Torr, the electron temperature was near 80 °K for times greater than a few hundred microseconds. At this very low pressure the rate of conversion of He^+ to He_2^+ is negligible compared to diffusion loss of He^+; recombination loss is also negligible. Thus, the rate of decay of He^+ is determined by ambipolar diffusion and hence by T_e. Mass-analyzed ion-wall currents indicated that $T_e = 80 \pm 15$ °K for $t > 300$ μsec, and $p = 0.2$ Torr.

Observation of atomic line and molecular band radiation from the plasma did not yield any additional quantitative information but its behavior did give additional support for the proposed plasma model. All band and line radiation behaved similarly and will be referred to simply as light. Atomic radiation from quantum levels greater than 4 was essentially absent. For purposes of illustration, consider a plasma in which the qss condition is satisfied (when this is not the situation, the light behaves somewhat differently but is still explainable by the model). When T_e was suddenly increased at $t = t_1$, the light level decreased to a relative minimum in a time less than the temporal resolution of the photon counting system (~1.5 μsec), and subsequently increased back to its nonheated level (see Fig. 3). This initial decrease in the light level is due to the T_e^{-X} dependence of the recombination rate. The subsequent rise in intensity back to its nonheated value is also explainable by the model because following the initial transient, the qss model once again applied [thus, $\alpha_0 N_{e0}^2(t) = \alpha_h N_{eh}^2(t) = S(t)$]. That is, the decreased recombination coefficient is compensated for by the increased electron density. This assumes that the intensity (I) is proportional to the rate of recombination.

When the microwave heating field was suddenly terminated at $t = t_2$, the light intensity I increased in a time less than 1.5 μsec and then subsequently decreased back to its nonheated value. This is explainable in the same manner as discussed above. We also find that

$$I(t_1^-)/I(t_1^+) = I(t_2^+)/I(t_2^-),$$

which is consistent with the qss model since the intensity reaches a maximum before N_e can change to any significant degree, and the initial change in αN_e^2, hence I, is governed only by the change in T_e.

VI. ANALYSIS OF ERRORS

The wall temperature of the discharge tube was assumed to be near 77 °K. Observation of the increase in gas pressure with periodic discharging showed that the average temperature of the walls did not rise by more than 1.5 °K at the fastest discharge rate used in this study.

The effective electron temperature T_e^* at various levels of microwave heating is illustrated in Fig. 9. Also shown is the value of T_e predicted by Margenau.[6] This data was obtained at a gas pressure of 30 Torr. The measured value of $T_e^* - 80$ is on the order of $\frac{1}{2}$ the value calculated by Margenau. [Frommhold's correction $F(Z)$ is small compared to the difference.] The reason for this discrepancy is not un-

derstood, although the effect of inelastic collisions with He_2^* is a possible candidate. An additional reason for this discrepancy may be that T_e^* does not accurately approximate the electron temperature. However, the observation that $T_e^* = 77 \pm 15$ °K for $t \gtrsim 600$ μsec (this time is slightly pressure dependent) indicates that this is not a likely cause for the discrepancy. The latter result is observed at all values of the sensing wave frequency. This indicates the absence of systematic error except possibly if T_e is significantly greater than 77 °K even for times greater than several milliseconds. In principle, an elevated T_e could be sustained by the energy input to the free electrons via the 5-eV electrons from the ionizing metastable-metastable collisions. However, a simple energy-balance analysis (for example, see Ingraham and Brown[20]) shows that for $p > 15$ Torr and $N_e < 10^{10}$ cm^{-3}, T_e should not be more than 2 °K higher than T_g. In this analysis the metastable density was estimated by the qss relation between N_e and $[M]$.

In light of the above, it appears that during the time of interest, for $p > 15$ Torr and in the absence of microwave heating, the electron temperature was near 80 °K. Thus, there is sufficient reason to believe that T_e^* is a reasonable approximation to T_e both with and without a microwave heating field.

The chief sources of error in the electron-density measurements are the inaccuracy of the phase-shift measurements $\Delta\Phi$ and the error involved in the evaluation of the filling factor ξ [see Eq. (2)]. We estimate that the measured N_e is accurate to ± 15% with all but 2% of this being systematic.

Additional error is introduced in the final evaluation of $\alpha_0^{(2)}$ and $\alpha_0^{(3)}$ because the initial time rate of change of $N_e(t_{1,2})$ must be evaluated, and the assumption must be made that T_e changes instantaneously at $t = t_{1,2}$. The time rate of changes of electron density at $t = t_{1,2}$ are consistently underestimated because they both decrease with increasing time. The measured values were corrected by the iterative procedure discussed in Sec. IV, but an additional ± 10% error is added to the values of $\langle \alpha_0^{(2)} \rangle$ and $\langle \alpha_0^{(3)} \rangle$ to account for possible under or over corrections.

The method used to evaluate $\alpha_0^{(2)}$ and $\alpha_0^{(3)}$ requires that the time rate of change of T_e at times $t_{1,2}^*$ is much greater than the rate of change of N_e. The time rate of change of T_e at $t = t_{1,2}^*$ is estimated as $1/\tau_e = \nu 2m/M$. If the criterion is set that the change in T_e must be 95% complete before N_e has changed by 10%, then it can be shown that this criterion is satisfied under the conditions of the experiment if $p > 2$ Torr.

Note must be made here of the results of Goldan and Goldstein[5] who measured τ_e at both 4.2 °K and 77 °K and found it to be much larger than that given by the expression $1/\tau_e = \nu 2m/M$. Their value was found from the rate of change of microwave absorptivity following termination of a microwave heating field. However, they did not account for a possible rapid change in N_e as was observed by Kaplafka[4] and in this work. Consequently, this raises some question about the validity of their reported values of τ_e. Thus, the conventional relation was used in this work as the criterion for equilibration time.

An additional ± 5% possible inaccuracy is added to the evaluated values of $\langle \alpha_0^{(2)} \rangle$ and $\langle \alpha_0^{(3)} \rangle$ to account for unforeseen systematic error. Adding to the aforementioned error limits, the standard deviation of the measured values, the value of α for He_3^+ with T_e near 80 °K is $(3.4 \pm 1.5) \times 10^{-6}$ cm^3 sec^{-1}.

The method used to evaluate $\alpha_0^{(1)}$ neglected the production of new atomic metastables via the recombination process. If recombination terminated in the atomic metastable state with unit probability and the qss relation for N_e was applicable, then β in Eq. (7b) should be replaced with an effective value equal to $\frac{1}{2}\beta$ (i.e., $\beta_{eff} = \frac{1}{2}\beta$). As a consequence of this recycling process, the determined $\alpha_0^{(1)}$ would be $\sqrt{2}$ times the value listed in Table II. Since termination of recombination in M surely occurs with less than unit probability, the necessary

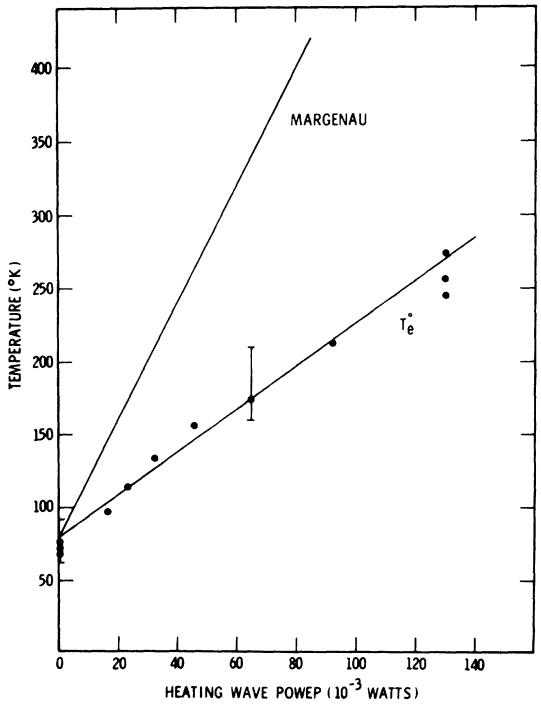

FIG. 9. Measured electron temperature T_e^* at various levels of microwave heating power. The bars represent maximum scatter limits. Also included is the value that T_e should have attained according to the theory of Margenau (Ref. 6).

correction to the listed values of $\alpha_0^{(1)}$ is definitely less than 41%. Thus, while the proper account of recycling could bring $\alpha_0^{(1)}$ into closer agreement with $\alpha_0^{(2)}$ and $\alpha_0^{(3)}$, to account for recycling would be meaningless in light of the factor of 2 accuracy limits on β.

Some experimental evidence is available which indicates that the recombination of He_3^+ is dissociative and results in an excited molecule. The dominance of molecular excited state densities over the corresponding densities in the atomic system is in agreement with f_3 being small. However, this observation alone is not conclusive evidence for $f_3 \ll 1$, especially since direct termination of He_3^+ recombination in M cannot be discounted. However, consider the possibility that f_3 may be significant. In this case $[M]$ at any time t depends on β, the initial metastable density, and on $\int_0^t \alpha(t) N_e(t)\, dt$. The recombination coefficient α is permitted to be time dependent to account for time-dependent perturbations which are applied to it. It would indeed be a coincidence to find that f_3 is large and that $[M]$ would in all cases be independent of the amplitude or duration of the perturbation, as was always observed in this study. As a consequence, it is believed that $f_3 \ll 1$ or expressed explicitly, $He_3^+ + e \rightarrow He_2^* + e$.

In the above error evaluation, the loss of electrons by diffusion to the walls has not been included. This is justified by calculations which indicate that diffusion loss is less than 1% of the recombination loss for $p > 5$ Torr, $N_e > 10^{10}$ cm^{-3}, and $T_e < 200$ °K. In addition, the behavior of the total light radiated from the plasma when T_e is altered by microwave heating indicated that diffusion could be neglected. In fact this behavior was used as a criterion for neglecting diffusion loss at elevated T_e and to set the maximum acceptable level of heating power at a given pressure.

An additional possible source of error can be attributed to our assignment of the effective recombination coefficient α^* to that of He_3^+, which requires that

$$\alpha_3 [He_3^+] \approx \sum \alpha_i [He_i^+].$$

It is reasonable to assume that $\alpha_3 > \alpha_{1,2}$, especially in light of previous measurements of $\alpha_{1,2}$ at $T_e = 300$ °K and our measured value of α^*. Since α^* also requires that $N_e [He_3^+] \approx N_e^2$, the assignment $\alpha^* = \alpha_3$ requires that $[He_3^+]/[He_2^+] \gg 1$. This latter ratio is amenable to mass-spectroscopy measurements at low gas pressure, but for $p > 10$ Torr the interpretation of the mass-spectroscopy results is complicated by questions concerning the plasma sampling as well as the behavior of the mass spectrometer at these higher pressures. These questions are not yet well enough understood to justify using the high-pressure mass-spectrometer results. The justification for assuming that the ratio $[He_3^+]/[He_2^+]$ is much greater than unity when the gas pressure is greater than 15 Torr is based on Patterson's[1] estimate of the lower limit for conversion of He_2^+ to He_3^+. The mass-spectrometer results of this study are consistent with Patterson's estimate for the latter reaction.

VII. SUMMARY

The electronic recombination coefficient of He_3^+ under thermalized conditions at a temperature near 80 °K is $(3.4 \pm 1.5) \times 10^{-6}$ cm^3 sec^{-1}. The electron-temperature dependence of this coefficient when the gas and ion temperatures are maintained at 80 °K is $T_e^{-\chi}$, $\langle \chi \rangle = 1.22$, $0.98 < \chi < 1.60$.

This study has also confirmed the observation by Kaplafka *et al.*[4] that in a 80 °K helium plasma, a small increase in electron temperature by means of microwave heating can result in a large increase in free-electron density. They attributed this increase in N_e to a T_e-dependent source term and suggested the existence of loosely bound electrons. The evidence presented here indicates that the new electrons result from metastable-metastable ionizing collisions. The increase in N_e upon application of a microwave field is accountable to an inverse T_e-dependent loss term for free electrons together with the T_e-independent source term.

ACKNOWLEDGMENTS

The authors would like to acknowledge helpful discussions with R. A. Gerber and other members of our group. They are also indebted to Professor L. Goldstein, University of Illinois, for his critical evaluation of several aspects of this work.

APPENDIX

In this Appendix we clarify the meaning of the effective collision frequency $\bar{\nu}_r$ which was used in the text and we outline the derivation of Eqs. (1) and (2).

A plasma immersed in an electromagnetic field alters the propagation characteristics of the wave according to its complex conductivity. The complex conductivity of a plasma at an angular frequency ω can be expressed as follows[21]:

$$\sigma = \sigma_r + j\ \sigma_i = -\frac{4\pi}{3} \epsilon_0 \omega_p^2 \int_0^\infty \frac{v^3}{\nu + j\omega} \frac{\partial f_0}{\partial v}\, dv, \quad \text{(A1)}$$

where f_0 is the spherically symmetric term in the expansion of the electron velocity distribution, $\nu = NvQ(v)$ is the velocity-dependent electron-neutral collision frequency for momentum transfer, and $\omega_p = N_e e^2 / \epsilon_0 m$ is the plasma angular frequency. Equation (A1) has been evaluated by Molmud[10] for several forms of $Q(v)$. For helium $[Q(v) = \text{const}]$ and $f_0(v)$ Maxwellian he obtained

$$\sigma = \epsilon_0 \omega_p^2 (\bar{\nu} - j\omega) / (\bar{\nu}^2 + \omega^2) , \tag{A2}$$

where

$$\bar{\nu} = \bar{\nu}_r + j\,\bar{\nu}_i$$

is a complex quantity;

$$\begin{aligned} \bar{\nu}_r &= \tfrac{4}{3}\,\nu\,[1 - 0.22\,(\nu/\omega)^2] , \\ \bar{\nu}_i &= 0.18\,(\nu^2/\omega)\,[1 + 2.14\,(\nu/\omega)^2] , \end{aligned} \tag{A3}$$

where $\nu = NQ\,(8kT/\pi m)^{1/2}$.

When the plasma conductivity is expressed by Eq. (A2) the solution for wave propagation in a uniformly filled waveguide is straightforward. However, with nonuniform filling, exact solutions are difficult and have been obtained in closed form only for a few special cases. Since to our knowledge the derivation of Eqs. (1) and (2) is not available in open literature, we outline below the perturbation solution used to obtain them.

A uniformly filled rectangular waveguide is excited in the dominant $TE_{1,0}$ mode[22] which has a propagation term $e^{[j\omega t - \Gamma z]}$. The propagation constant Γ is obtained by solution of the wave equation with the appropriate boundary condition and the condition that the medium filling the waveguide is completely described by its complex conductivity

$$\Gamma^2 = [j\omega\mu_0(\sigma + j\omega\epsilon) + (\pi/a)^2] = (\alpha + j\beta)^2 , \tag{A4}$$

where a is the broad dimension of the waveguide. Equating real and imaginary parts of Eq. (A4) the following expressions are obtained:

$$\omega\mu_0\sigma_r = 2\alpha\beta , \quad \omega\mu_0\sigma_i = \beta^2 - \alpha^2 - \beta_0^2 , \tag{A5}$$

where $\beta_0 = [\omega\mu_0\epsilon_0 - (\pi/a)^2]$ is the propagation constant for $\sigma = 0$ and is related to the guide wavelength λ_{g0} by $\beta_0 = 2\pi/\lambda_{g0}$. The phase shift in degrees $\Delta\Phi^\circ$ and the attenuation in decibels Δ dB for a length l of plasma are related to α and β by the following:

$$\begin{aligned} \Delta\ \mathrm{dB} &= 10 \ln e^{2\alpha l} = 8.68\,\alpha l , \\ \Delta\Phi^0 &= \tfrac{1}{2}(360/\pi)\,(\beta_0 - \beta)\,l. \end{aligned} \tag{A6}$$

Substitution of Eqs. (A6) into Eqs. (A5) yields

$$\sigma_r = \omega\epsilon_0 \frac{\lambda^2}{\lambda_{g0}} (0.115) \frac{\Delta\,\mathrm{dB}}{\pi l} [1 - \Theta], \tag{A7a}$$

$$\sigma_i = \omega\epsilon_0 \left(\frac{\lambda}{\lambda_{g0}}\right)^2 \left(\Theta^2 - 2\Theta - \frac{\Delta\ \mathrm{dB}\ \lambda_{g0}}{8.68\, l\, 2\pi}\right) , \tag{A7b}$$

where

$$\Theta = \frac{\Delta\Phi^0 \lambda_{g0}}{360\, l} .$$

Application of Eq. (A2) results in the following expressions for $\bar{\nu}_r$ and ω_p^2:

$$\bar{\nu}_r = \frac{(0.115)\ \Delta\mathrm{dB}\ \lambda_{g0}\omega}{\pi l} \left(\frac{1 - \Theta}{2\Theta - \Theta^2}\right) , \tag{A8a}$$

$$\omega_p^2 = \left(\frac{\lambda}{\lambda_{g0}}\right)^2 \omega^2 \left(2\Theta - \Theta^2\right) \left(\frac{(\bar{\nu}_r/\omega)^2 + (1 + \bar{\nu}_i/\omega)^2}{1 + \bar{\nu}_i/\omega}\right). \tag{A8b}$$

The last term in Eq. (A7b) has been neglected. For small phase shifts (i.e., $\Theta \ll 1$) Eq. (A8a) reduces to

$$\bar{\nu}_r = 41.4\,\frac{\Delta\ \mathrm{dB}}{\Delta\,\Phi^0}\,f . \tag{A9}$$

For all cases of interest in this work ν/ω was less than 0.5. Consequently, $\bar{\nu}_i/\omega \ll 1$ and expansion of the bracketed term in Eq. (A8b) shows that the quantity $\bar{\nu}_i/\omega$ can be neglected in comparison with $(\bar{\nu}_r/\omega)^2$. Thus, for the plasmas studied here

$$\omega_p^2 \approx \left(\frac{\lambda}{\lambda_{g0}}\right)^2 2\Theta \left(\bar{\nu}_r^2 + \omega^2\right). \tag{A10}$$

Solutions similar to those expressed by Eqs. (A9) and (A10) can be obtained for a partially filled waveguide by a perturbation solution. The fields in the waveguide are assumed to be unaffected by the plasma except for their propagation constant, the spatial distributions of the fields remaining unchanged. The propagation constant is obtained with the aid of the energy conservation equation. This results in equations identical to Eqs. (A5) except the real and imaginary components of the complex conductivity are replaced by their spatially averaged values

$$\langle\sigma_{i,r}\rangle = \int_{S_g} \sigma_{i,r} E_y^2\,dx\,dy \Big/ \int_{S_g} E_y^2\,dx\,dy , \tag{A11}$$

where E_y is the wave electric field, (x, y) are transverse spatial coordinates, and the integral is evaluated over the waveguide cross section S_g. If both σ_i and σ_r are spatially uniform inside the discharge tube and zero outside the tube, then

$$\langle\sigma_{i,r}\rangle = \sigma_{i,r} \left(\int_{S_j} E_y^2\,dx\,dy \Big/ \int_{S_g} E_y^2\,dx\,dy\right) = \sigma_{i,r}\,\xi ,$$

where the integral in the numerator is evaluated over the tube cross-sectional area S_j. With this modification, Eq. (A9) is applicable for a partially filled waveguide but Eq. (A10) must be multiplied by a factor $1/\xi$:

$$\omega_p^2 = \frac{1}{\xi} \left(\frac{\lambda}{\lambda_{g0}}\right)^2 2\Theta \left(\bar{\nu}_r^2 + \omega^2\right) . \tag{A12}$$

Applicability of this perturbation solution requires that $\omega_p^2 \ll \omega$ or $\Theta \ll 1$ and $\bar{\nu}_i/\omega \ll 1$.

*Work supported by the U. S. Atomic Energy Commission.

[1]P. L. Patterson, J. Chem. Phys. 48, 3625 (1968).
[2]E. E. Ferguson, F. C. Fehsenfeld, and A. L. Schmeltekopt, *Advances in Atomic and Molecular Physics*, edited by D. R. Bates and Immanuel Estermann (Academic, New York, 1969), Vol. 5, Chap. 1, p. 46.
[3]C. P. deVries and H. J. Oskam, Phys. Letters 29A, 299 (1969).
[4]J. P. Kaplafka, H. Merkelo, and L. Goldstein, Phys. Rev. Letters 21, 970 (1968).
[5]P. D. Goldan and L. Goldstein, Phys. Rev. A138, 39 (1965).
[6]H. Margenau, Phys. Rev. 69, 508 (1946).
[7]H. Hermansdorfer, *Plasma Diagnostics*, edited by W. Lochte-Holtgreven (North-Holland, Amsterdam, 1968), Chap. 8, p. 478.
[8]L. Goldstein, in *Advances in Electronics and Electron Physics*, edited by L. Marton (Academic, New York, 1955), Vol. 7.
[9]J. M. Anderson and L. Goldstein, Technical Report No. 7, AFCRC Contract No. AF19(604)-524, Electrical Engineering Research Laboratory, University of Illinois, 1955 (unpublished).
[10]P. Molmud, Phys. Rev. 114, 29 (1959).
[11]H. S. W. Massey and E. H. S. Burhop, *Electronic and Ionic Impact Phenomena* (Oxford U. P., Oxford, England 1969), Vol. 1, Chap. 2, p. 83.
[12]Lothar Frommhold, Manfred A. Biondi, and F. J. Mehr, Phys. Rev. 165, 161 (1968).
[13]A. V. Phelps and J. P. Molnar, Phys. Rev. 89, 1202 (1953).
[14]W. A. Fitzsimmons, N. F. Lane, and G. K. Walters, Phys. Rev. 174, 193 (1968).
[15]Paul L. Patterson, Joint Institute for Laboratory Astrophysics, Report No. 87, University of Colorado, 1966 (unpublished).
[16]E. C. Beaty and P. L. Patterson, Phys. Rev. A137, 346 (1965).
[17]D. R. Bates, A. E. Kingston, and R. W. P. McWhirter, Proc. Roy. Soc. (London) 267, 297 (1962).
[18]Jacques Berlande, Michel Cheret, Robert Deloche, Alain Gonfalone, and Claude Manus, Phys. Rev. A 1, 887 (1970).
[19]A. V. Phelps (private communication).
[20]J. C. Ingraham and Sanborn C. Brown, Phys. Rev. A138, 1015 (1965).
[21]A. V. Phelps, O. T. Fundingsland, and Sanborn C. Brown, Phys. Rev. 84, 559 (1951).
[22]Edward C. Jordan, *Electromagnetic Waves and Radiating System* (Prentice-Hall, Englewood Cliffs, N. J., 1950), Chap. 9.

PHYSICAL REVIEW A VOLUME 3, NUMBER 1 JANUARY 1971

Inelastic Scattering of Electrons and Protons by the Elements He to Na†

Eugene J. McGuire
Sandia Laboratories, Albuquerque, New Mexico 87115
(Received 16 July 1970)

We have calculated discrete and continuum generalized oscillator strengths for all the occupied shells of He–Na and the 3*s* and 3*p* continuum generalized oscillator strengths for Ar. The calculations are done with a one-electron common-central-potential unrelaxed-core approximation. The generalized oscillator strengths were used to compute proton-excitation and -ionization cross sections and stopping power, electron-ionization cross sections, and neutral-neutral-ionization and -stripping cross sections. For proton ionization above 200 keV and electron ionization above 200 eV, the calculated cross sections are in better than 20% agreement with experiment. The calculated proton stopping power is lower than experiment by 25% at 100 keV and within 10% at 1 MeV. The computed He-He ionization cross section agrees with the measurement by Wittkower, Levy, and Gilbody, while the computed He-Ar ionization cross section is a factor of 5 higher than the measurement by Puckett, Taylor, and Martin.

I. INTRODUCTION

The generalized oscillator strength was introduced by Bethe[1] and used in his stopping-power theory.[1,2] Bethe's stopping-power formula uses the optical oscillator strength, and for many years the generalized oscillator strength remained unexplored. Lassettre's[3] electron scattering experiments provided the first extensive experimental measurements of atomic and molecular generalized oscillator strengths. These experimental generalized-oscillator-strength measurements have been applied by Green and Peek[4] to certain molecular scattering problems. Rau and Fano[5] have obtained asymptotic properties of generalized oscillator strengths. Inokuti and Kim[6] and Oldham[7] have done accurate calculations of generalized oscillator strengths for a limited number of discrete excitations in He. Bell, Kingston, and Kennedy[8] have done similar calculations for a wider range of discrete excitations with a less accurate ground-state wave function. Bell and Kingston[9] have done proton and electron ionization for He, and Oldham[10] has done proton ionization for He.

Our purpose is to use the generalized-oscillator-strength (GOS) approach in calculations for a wide